

scheduled for ApJ, vol. 515, April 10, 1999

## The initial stellar mass function from random sampling in hierarchical clouds II: statistical fluctuations and a mass dependence for starbirth positions and times

Bruce G. Elmegreen<sup>1</sup>

### ABSTRACT

Observed variations in the slope of the initial stellar mass function (IMF) are shown to be consistent with a model, introduced previously, in which the protostellar gas is randomly sampled from clouds with self-similar hierarchical structure. RMS variations in the IMF slope around the Salpeter value are  $\pm 0.4$  when only 100 stars are observed, and  $\pm 0.1$  when 1000 stars are observed. Similar variations should be present in other stochastic models too.

The hierarchical-sampling model reproduces the tendency for massive stars to form closer to the center of a cloud, at a time somewhat later than the formation time of the lower mass stars. The systematic variation in birth position results from the tendency for the trunk and larger branches of the hierarchical tree of cloud structure to lie closer to the cloud center, while the variations in birth order result from the relative infrequency of stars with larger masses.

The hierarchical cloud sampling model has now reproduced most of the reliably observed features of the cluster IMF. The power law part of the IMF comes from cloud hierarchical structure that is sampled during various star formation processes with a relative rate proportional to the square root of the local density. These processes include turbulence compression, magnetic diffusion, gravitational collapse, and clump or wavepacket coalescence, all of which have about this rate dependence. The low mass flattening comes from the inability of gas to form stars below the thermal Jeans mass at typical temperatures and pressures. The thermal Jeans mass is the only relevant scale in the problem. Considerations of heating and cooling processes indicate why the thermal Jeans mass should be nearly constant in normal environments, and why this mass might increase in starburst regions. In particular, the relative abundance of high mass stars should increase where the average density of the interstellar medium is very large; accompanying this increase should be an increase in the average total efficiency of star formation. Alternative models in which the rate of star formation is independent of density and the local efficiency decreases systematically with increasing stellar mass can also reproduce the IMF, but this is an adjustable result, not a fundamental property of hierarchical cloud structure, as is the preferred model.

The steep IMF in the extreme field is not explained by the model but other origins are suggested, including one in which massive stars in low pressure environments halt other star formation in their clouds. In this case, the slope of the extreme field IMF is independent of the slope of each component cluster IMF, and is given by  $(\gamma - 1)/\alpha$  for cloud mass function slope  $-\gamma \sim -2$  and power law relation,  $M_L \propto M_c^\alpha$ , between the largest star in a low-pressure cloud,  $M_L$ , and the cloud mass,  $M_c$ . A value of  $\alpha \sim 1/4$  is required to explain the extreme field IMF as a superposition of individual cluster IMFs. We note that the similarity between cluster IMFs

---

<sup>1</sup>IBM Research Division, T.J. Watson Research Center, P.O. Box 218, Yorktown Heights, NY 10598, USA,  
bge@watson.ibm.com

and the average IMF from global studies of galaxies implies that most stars form in clusters and that massive stars do not generally halt star formation in the same cloud.

Subject headings: stars: formation – stars: mass function – ISM: structure

## 1. Introduction

The initial stellar mass function (IMF) is approximately a power law for intermediate (Salpeter 1955) to large masses (see review in Massey 1998), but it flattens at low mass (Miller & Scalo 1979; Kroupa, Tout & Gilmore 1990; see review in Reid 1998), often down to the limit of detection, which is sometimes as low as  $0.1M_{\odot}$  or lower (see reviews in Lada, Lada & Muench 1998; Scalo 1986, 1998). Such flattening is widely observed for Milky Way disk stars, and it is also inferred for halo, bulge, and globular cluster stars (see reviews by Cool 1998 and Wyse 1998).

This flattened power-law IMF applies to a wide variety of regions, although the details vary. For example, the mass at the threshold of the flat part seems to be higher in starburst regions (Rieke et al. 1980, 1993; see reviews in Scalo 1990a; Zinnecker 1996; Leitherer 1998), giving a larger proportion of high mass stars compared to the Solar neighborhood. The cluster in 30 Doradus may have a higher threshold mass too (Nota 1998). The result for starburst galactic nuclei comes from the observation that the luminous mass from young massive stars is not much smaller than the dynamical mass from the rotation curve, so there cannot be much mass in the form of low mass stars (Wright et al. 1988; Telesco 1988; Doane & Matthews 1993; Doyon, Joseph, & Wright 1994; Smith et al. 1995). However, Satyapal (1995,1997) found that the high mass stars in the classical starburst galaxy M82 are spread out over a large area, in which case the normal proportion of low mass stars could be present. Other evidence for normal IMFs in starburst regions is in Devereux (1989), Schaerer (1996) and Calzetti (1997). The result for 30 Dor comes from stellar counting, and if confirmed, would be the first direct evidence for this effect.

There is also an observation that the largest clouds produce the largest stars, as if the IMF depends on cloud mass (Larson 1982). This result is analogous to the statement that spiral arm clouds, which tend to be large, produce proportionally more massive stars than interarm clouds (Mezger & Smith 1977) which tend to be small. These concepts, along with massive-star triggering scenarios, led to suggestions of a bi-modal IMF (Eggen 1976, 1977; Elmegreen 1978; Güsten & Mezger 1983; Larson 1977, 1986).

The proportion of high and low mass stars may differ for cluster and field populations too, in the sense that the slope of the local field star IMF may be steeper than the slope of the cluster IMF (see discussion in Elmegreen 1997, hereafter Paper I, and 1998). This is the case for intermediate mass stars in the solar neighborhood (Scalo 1987) and in an extreme field region of the LMC (Massey et al. 1995).

The most massive stars might also be born slightly closer to a cloud's center than the low mass stars. In the Orion trapezium region, Hillenbrand & Hartmann (1998) found such a distribution and suggested the stars must have been born this way because the cluster is too young to have relaxed after an initially random birth order (see also Jones & Walker 1988; Hillenbrand 1997; Bonnell & Davies 1998). High mass stars are also concentrated in NGC 2157 (Fischer et al. 1998), SL 666, and NGC 2098 (Kontizas et al. 1998). This relative concentration of high mass stars in clusters has been suspected for a long time on the basis of color and IMF variations (Sagar & Bhatt 1989; Pandey, Mahra, & Sagar 1992; Vazquez et al. 1996). In addition, the massive stars in a cluster might be born later than the low mass stars (Herbig 1962; Iben & Talbot 1966), as recently suggested for 30 Dor (Massey & Hunter 1998).

These systematic variations in the IMF are distinct from the seemingly random fluctuations from cluster to cluster. In a recent review, Scalo (1998) pointed out that while the average slope of the IMF at intermediate to high mass is about the value found originally by Salpeter, i.e.,  $-1.35$  for stellar counting in equal logarithmic intervals, the slopes for individual regions vary by  $\pm 0.5$ . It is currently unknown if these variations result from physical differences in the intrinsic IMFs for each region, or from statistical fluctuations around a universal IMF. The extreme cases certainly look non-random since they have smooth power law IMFs with slopes that are significantly different from the Salpeter value. For example, Brown (1998) found an IMF slope in the Orion association of  $\sim -1.8$ , using Hipparcos data to determine membership combined with photometry to determine masses, while Massey (1998) and collaborators get a fairly consistent value of  $\sim -1.35$  for high mass stars in most associations in the Large Magellanic Cloud and the Milky Way, using spectroscopy to determine masses. The difference between these two results might be from the different methods used to determine mass (Massey 1998), or they could be from different physical processes of star formation. Another extreme example is the Pleiades IMF (Meusinger et al. 1996), with its slope of  $\sim -2.3$  (see discussion in Scalo 1998). Such steep slopes for clusters (see also NGC 6231 – Sung, Bessel, & Lee 1998) are troublesome because they could arise from mass segregation and not IMF differences (e.g., see Pandey, Mahra, & Sagar 1992).

The purpose of the present paper is to consider some of these variations using the model introduced in Paper I. We contend that not all of the variations result from physical differences: some probably reflect sampling limitations in the observations, others may result from incorrect assumptions in the interpretation, and still others might be purely statistical in nature. Yet some variations seem real and we would like to explain them, as well as the statistical effects, with a minimum of assumptions.

Other theories of the IMF were reviewed by Cayrel (1990) and Clarke (1998). A review of both observations and theory is in Elmegreen (1999). The closest models to the present were by Henriksen (1986, 1991) and Larson (1992). Henriksen used the size distribution function for structures in a fractal of dimension  $D$ , given as  $n(R)d\log R \propto R^{-D}d\log R$  by Mandelbrot (1983), and assumed that the density  $\rho$  varies with size as observed in self-gravitating clouds,  $\rho \propto R^{-1}$ . This gave a mass function for cloud structure that agreed well with observations if  $D \sim 2.7$ . Larson (1992) also used the size distribution for a fractal, and assumed that final stellar mass is proportional to the linear size of the cloud piece. Then the slope of the IMF in linear intervals becomes  $1 + x = 1 + D \sim 3.3$  for  $D = 2.3$ . This IMF is steeper than the Salpeter IMF, which has  $1 + x = 2.3$ , but Larson suggested that perhaps stars form in subparts of clouds where  $D$  is smaller than 2.3, or that larger structures have larger temperatures, which would break the assumed linear relationship between star mass and scale size.

The present model is similar to these in the suggestion that the power law part of the IMF comes from cloud geometry. It is similar to Larson's model also because of the assumption that the lower mass limit is related to the thermal Jean's mass. However, the present model differs from the others in several important respects. First, the star mass is assumed to be proportional to the cloud mass here, rather than linear size, so we are not constrained to assume filamentary cloud pieces. Second, the density structure of the cloud is given by the hierarchy, consistent with the number-size relation, not by the density structure of a self-gravitating cloud. As a result, the IMF in the present model has a power law that depends only weakly on the fractal dimension of the cloud, unlike the other models, and yet agrees with the observed IMF in spite of a nearly complete absence of free parameters.

We return to a discussion of the present model in Section 4. In the next section, the various observations of the IMF are reviewed in more detail in order to assess which are likely to be the result of physical effects, and which are likely to come from statistical sampling.

## 2. Sorting out what's real

The observation that high mass clouds produce high mass stars is the type of effect that can arise from sampling statistics: larger clouds produce more stars, so the IMF is sampled further out in the high mass tail, giving a more massive, highest-mass star (Larson 1982). Indeed, the statistical trend that is expected from random sampling matches the observations well (Elmegreen 1983), so there is little room for further effects based on physical variations (although see Khersonsky 1997). Similarly, the inference that spiral arm clouds produce proportionally more massive stars than interarm clouds should contain the same sampling effect based on cloud mass, but in addition, could contain an observational problem that low mass stars are too faint to see in distant spiral arm clouds.

Along these same lines, we also expect the most massive stars to form last in a cluster because they are rare and unlikely to appear until after several thousand lower mass stars form first (Elmegreen 1983).

The difficulty in observing low mass stars may account for some of the inference that starburst regions have truncated IMFs, but if the truncation is severe and based on either direct star counts above the sensitivity limits, or on luminous mass compared to dynamical mass, then the argument is difficult to interpret any other way.

The difference between field star IMFs and cluster IMFs is more difficult to assess because both data are often of comparable quality, and because there are three distinct types of observations that have led to this conclusion. One is a comparison between the Solar neighborhood field-star IMF (Scalo 1986; see also Tsujimoto et al. 1997 for a discussion of metallicity yields and the field star IMF) or the LMC field star IMF (Parker et al. 1998), and essentially all other IMFs measured in associations (Massey 1998). Another is a comparison between IMFs of clustered star-forming regions in low and high density environments (J.K. Hill et al. 1994; R.S. Hill et al. 1995; Massey et al. 1995). The third is a comparison between high and low mass young star counts in high and low density regions of the same cloud (Ali & DePoy 1995).

In the first case, there are corrections to the Solar field population at low and intermediate mass that do not arise in young clusters – corrections to account for stellar evolution, such as the loss of evolved stars and possible variations in the past star formation rate (Scalo 1986). There are also corrections to account for the systematic increase in stellar scale height with age (Scalo 1986). These same corrections arise at high mass too, but the time scales for evolution and star formation variations are much smaller for high mass stars, and the scale height effect could be erratic because of the small number of stars involved. For example, at intermediate to high mass, one might conjecture that the field star IMF is a composite of several different cluster IMFs from aging dispersed associations in the Solar neighborhood. Perhaps all of these local stars are from Gould's Belt, with different ages, degrees of dispersal, and initial distances from the plane for each former association. Then the Solar field star IMF at intermediate and/or high mass could be steeper than the IMF in each cluster if the low mass stars systematically drift further from their points of origin than higher mass stars (because of the greater ages of low mass stars), or if older clusters that have no massive stars anymore (e.g., the Cas-Tau association) happen to be closer to us than younger clusters that still have most of these stars (e.g., Perseus, Sco-Cen and Orion).

In the second case, there could be some effect from differential drift as well, although Massey et al. (1995) contend that the extreme-field regions in the LMC, in which star formation occurs more than 30 pc from catalogued OB association boundaries, are too far from other clusters for low mass contamination by differential drift to be important in the IMF. This is puzzling since Massey & Hunter (1998) found essentially the same IMF in clusters with a wide range of densities. Thus, either the IMF is independent of

star-forming density, and the extreme field is somehow not a representative sample, or there is a threshold low density where the IMF abruptly changes from Salpeter-like to something much steeper at lower density.

There is probably no evolutionary effect to explain the third case, because the entire cloud is young, so differential drift does not seem possible unless low mass stars move faster than high mass stars. On the other hand, one might expect different IMFs in low and high density regions of molecular clouds for the same reason that massive stars form closer to the center of a cluster than low mass stars (Hillenbrand & Hartmann 1998).

The last type of IMF variation discussed above, i.e., the scatter in the slope of the IMF from cluster to cluster, is again something that might be expected from statistical sampling. This is amenable to test because one can look for a correlation between the numbers of stars used to determine each IMF and the deviations of the slopes from the average value for all clusters. If the slope deviation systematically decreases for increasing numbers of stars, then the slope fluctuations could be random. Otherwise, there is good reason to look for systematic physical differences that give rise to the different slopes.

We interpret these observations to indicate that, at the present time, there are four distinct physical effects that have to be explained by a theory of the IMF: (1) the power-law slope at intermediate to high stellar mass, with a value close to that found by Salpeter (1955); (2) the flattening at low mass for clusters and star-forming regions in our Galaxy; (3) the increase in the transition mass between power-law and flat regions of the IMF in starburst galaxies and 30 Dor, and (4) the preferential birth of high mass stars close to cluster centers. We also expect the theory to produce three additional effects for statistical reasons: (1) the tendency for the largest mass star in a region to increase with the total number of stars, (2) the tendency for the largest mass stars to form last, and (3) the seemingly random variations in the intermediate and high mass IMF slopes from region to region.

The first three of these physical effects, and the first of the statistical effects, were demonstrated for our model in Paper I. They will be discussed here again briefly in Section 2. The fourth physical effect and the third statistical effect were not known at the time Paper I was written, so they will be discussed here. The second statistical effect has received recent attention by Massey & Hunter (1998), so it will be discussed here as well. We show that the same IMF model is consistent with all three statistical and four physical effects, but the observation of the fourth physical effect is not matched well by the model. There is some need for an additional physical process, such as a reasonable enhancement in cloud condensation from self-gravity. This would alter the internal structure of the cloud from a purely self-similar hierarchical cloud, as assumed by the model so far, to a centrally condensed structure. Such an alteration would not affect the other attributes of the IMF model, including the *relative order* of birth locations of stars in a cluster, but it would affect the *absolute* birth locations as the cloud structure becomes condensed in the center.

There could also be a physical effect that limits the masses of the largest stars that form, but such a mass limit has apparently not been observed yet (e.g., Massey & Hunter 1998), so we do not consider it in the model. Demonstration of a mass limit like this would require the observation of an IMF out to very high masses, with a statistically significant number of “highest” mass stars and an abrupt drop in the number of stars with higher masses.

### 3. The extreme field IMF

The IMF model developed here and in Paper I cannot explain the steep slope of the high-mass IMF observed in some extreme field studies (Massey et al. 1995) without considering significantly different physical effects. Massey et al. define the extreme field as regions of star formation more than 30 pc from cataloged OB associations. The extreme field regions of the Milky Way are not the same as the local field, which contains a mixture of stars that were likely to have formed in standard clusters.

Two possible explanations for the steep IMF in the extreme field come to mind. One is a systematic decrease in the efficiency of star formation for increasing clump mass in the case of extreme field star formation, but not clustered star formation. This is considered again in Section 8. This situation might arise if there is a transition at extremely low pressure, such that in low pressure environments, all stars destroy their clouds with increasing effectiveness at increasing mass, but in high pressure environments, stars do not destroy their clouds much at all, unless they are stellar types O or B.

As an example of this effect, consider a field IMF that is a superposition of IMFs from many star-forming clouds, all with different masses, and consider that the largest stellar mass in each cloud increases with the cloud mass, perhaps because it takes a more massive star to destroy a more massive cloud. If  $M_L$  is the largest stellar mass and  $M_c$  is the cloud mass, then we can write this condition as  $M_L \propto M_c^\alpha$ . Because many clouds, even small clouds, can produce low mass stars, but only the larger clouds produce high mass stars, the summed IMF will be steeper than the individual cloud IMFs. If the individual cloud IMF is  $n(M)dM = n_0 M^{-1-x} dM$ , then  $n_0 = x M_L^x$  so there is one star with the largest mass (i.e.,  $\int_{M_L}^{\infty} n(M)dM = 1$ ). The summed IMF from all the clouds is  $n_{sum}(M)dM = n(M) \int_M^{\infty} P(M_L)dM_L$ , where  $P(M_L)dM_L$  is the probability distribution for the largest mass, which is given by  $P(M_L)dM_L = N(M_c)dM_c$  for cloud mass distribution  $N(M_c) \propto M_c^{-\gamma}$ . With the above relation between  $M_L$  and  $M_c$ ,  $P(M_L)$  gets converted to  $P(M_L)dM_L \propto M_c^{-\gamma} (dM_c/dM_L) dM_L$ , which gives  $P(M_L) \propto M_L^{(1-\gamma-\alpha)/\alpha}$ . Thus the integral for  $n_{sum}$  can be evaluated, with the result that  $n_{sum}dM \propto M^{-1-x_{eff}} dM$  for effective  $x_{eff} = (\gamma - 1)/\alpha$ . Note that the summed IMF from all the clusters is independent of the IMF of each cluster (i.e.,  $x_{eff}$  is independent of  $x$ ).

What are  $\gamma$  and  $\alpha$ ? The power in the cloud mass function is  $\gamma \sim 2$ , considering all possible levels in the cloud hierarchy, as before, and the power in the  $M_L(M_c)$  relation presumably comes from cloud destruction. According to the molecular cloud scaling relationships (Larson 1981), the binding energy of a molecular cloud,  $GM_c^2/R$ , is proportional to radius  $R^3$  since  $M_c \propto R^2$ . Presumably an embedded cluster has to liberate a cloud binding energy in a multiple of the crossing time in order to destroy it without significant energy dissipation. Thus the cloud destructive power of the embedded cluster has to exceed  $(GM_c^2/R) (GM_c/R^3)^{1/2} \propto M_c^{5/4}$ . This result assumes that low-pressure environments produce clouds with the same scaling relations as normal star-forming environments. To get the extreme field IMF, we need  $\alpha \sim 0.25$ , so the cluster destructive power has to scale with the fifth power of the largest stellar mass. Then the summed IMF has  $x_{eff} \sim (\gamma - 1)/\alpha \sim 4$ , which is about what Massey et al. (1995) see in the field regions of the LMC and Milky Way. There are no observations of  $\alpha$  in the extreme field, so this explanation requires confirmation. The steep slope of the relation between cluster destructive power and largest stellar mass might arise for clusters whose largest star is at the transition between A-type and B-type; this is where the primary agent for cloud destruction changes from pre-main sequence winds to ionization.

Note that in clustered regions, the IMF is about the same as in the Solar neighborhood field, and also the same as the summed IMF in whole galaxies, i.e., all have  $x \sim 1.3 - 1.8$ . This means not only that most stars form in clusters and not the extreme field, but also that *the most massive stars do not halt star*

formation in their clouds by destroying the clouds. If they did, then the summed IMF would be steeper than the individual cluster IMFs (for further discussion of this point, see the review in Elmegreen 1999).

Another physical difference that could affect the IMF in the field would be a difference in the type of star-forming cloud in low and high density environments. Presumably low-density star-forming regions have only small star-forming clouds, like the Taurus clouds, or only low-density clouds, like the Maddalena & Thaddeus (1985) cloud. Such clouds may be systematically different than high-mass, high-density clouds, such as those found in OB associations. It is possible, for example, that low self-gravity and low central pressure allow low-mass or low-density clouds to be more filamentary than high-mass or high density clouds. In that case, gravitational instabilities along the filaments can produce a *characteristic* mass for dense globules (Tomisaka 1996), and stars forming in these globules (Nakamura et al. 1995) could produce a delta-function IMF centered at some fraction of the globule mass. Such an IMF would be very steep for high mass stars.

#### 4. Introduction to the theory

A theory for the IMF based on random sampling in hierarchically structured clouds has already been shown to have several of the requirements discussed above (Paper I). The Salpeter slope comes from two assumptions: (1) that star mass follows gas mass, and (2) gas turns into stars at a rate proportional to some modest power of the local gas density, such as a square root. This would be the case for gravitational, magnetic diffusion-regulated, or turbulent processes, as well as for clump-collision processes, considering the molecular cloud scaling laws (see appendix). The low mass flattening comes from a third assumption: (3) that gas clumps smaller than the thermal Jeans mass,  $M_J \sim (k_B T / m_{H_2})^2 / (G^3 P)^{1/2}$ , at the temperature  $T$  and pressure  $P$  of the star-forming part of the cloud do not readily form stars because they cannot ever become strongly self-gravitating.

Assumption (3) was claimed to be the reason why the transition mass between the flat and power-law parts increases for starburst regions. There the quantity  $T^2 / P^{1/2}$  presumably increases because of an increase in  $T$  with the higher radiation fields (offsetting the known increase in  $P$  for these regions). We also showed in Paper I, without any other assumptions, how stochastic effects cause the mass of the largest star to increase with the number of stars formed, which is the first statistical effect mentioned above. Here we show that the theory reproduces the observed level of fluctuations in the IMF slope from region to region, as compiled by Scalo (1998), and we reproduce the observation that high mass stars form closer to a cluster center than low mass clouds (Hillenbrand & Hartmann 1998). We also show that high mass stars tend to form last in a stochastic model like this.

The ratio  $T^2 / P^{1/2}$  that appears in the thermal Jeans' mass should not vary much if the molecular cloud heating rate from starlight and cosmic rays scales with the local stellar column density in the disk. This is because molecular cloud cooling scales roughly with  $T^2$  to  $T^3$  (Neufeld, Lepp, & Melnick 1995), so the numerator in the expression  $T^2 / P^{1/2}$  varies almost directly with the local gas surface density of stars, and because the interstellar pressure scales roughly with the square of the disk column density, so the denominator in this expression also varies with the local stellar surface density. Only when the star formation rate is very high per unit gas mass, as in starburst regions, will the heating luminosity per unit gas mass increase substantially, thereby increasing  $T^2$  more than  $P^{1/2}$  to shift the “characteristic” or minimum mass of star formation upward. This increase in star formation rate per unit gas mass is expected at high average gas density, because the star formation rate scales with a power of the gas density that is greater

than 1 (Kennicutt 1998). Thus the peak in the IMF should shift toward higher mass in star-forming regions with very high ambient gas density. Note that this implies that *the global efficiency of star formation should increase directly with the minimum stellar mass*. Similarly, the global gas consumption time should vary with the inverse of the minimum stellar mass. Other than this physical variation of the low mass flattening limit with  $T^2/P^{1/2}$ , the IMF should be “universal” according to this theory, with statistically reasonable fluctuations that depend on the number of stars sampled.

The model requires very few physical assumptions, yet many of the physical processes that lead to star formation should be important for the final stellar mass. Can the IMF really be so independent of the processes of star formation? Of course, star formation is not purely random as in the model: stars form when and where they do for physical reasons. Indeed, the more we know about star-formation, the more we will be able to say that a particular star formed for a particular reason. We can say this for many stars already: there are known triggering processes that form stars in well observed regions, either one star at a time (as in pressurized globules) or in groups (as at the periphery of HII regions; see the review of triggering processes in Elmegreen 1998). These observations make random sampling models unnecessary. However, the model uses random sampling only as a mathematical tool: there is an underlying assumption that the mixture of real triggering processes is about the same everywhere once more than several hundred stars are formed. This means that the same fraction of stars forms by globule squeezing, or clump collisions, or gravitational collapse along filaments, or whatever the process might be, in all regions *on average*. If this is the case, then we do not have to say how a particular star formed in order to explain the IMF. By the time all of these star formation processes are *reduced* to the IMF, by gross averaging, essentially all of the important physical details have been lost. In this sense, the IMF model is not a theory of star formation, nor does it contain a theory of star formation. It is only a representation of how a large number of processes can combine to give an average stellar mass distribution that is subject to only a few reasonable physical constraints, such as the basic structure of clouds and the expected lower mass limit from cloud self-gravity.

An important assumption of the model is that star-forming cores generate, or preserve from some previous state, a hierarchical structure that is similar to what is commonly observed in non-star-forming clouds, e.g., as fractal structure along molecular and atomic cloud edges (Beech 1987; Bazell & Désert 1988; Scalo 1990b; Dickman, Horvath, & Margulis 1990; Falgarone, Phillips, & Walker 1991; Falgarone, Puget & Perault 1992; Zimmermann & Stutzki 1992, 1993; Henriksen, 1991; Hetem & Lepine 1993; Vogelaar & Wakker 1994; Pfenniger & Combes 1994; Fleck 1996; Elmegreen & Falgarone 1996; Falgarone & Phillips 1997; Stutzki et al 1998). Hierarchical structure is critical to the theory, yet it is not directly confirmed by observations of cluster-forming cores. Indeed, most stars form in clusters (Lada, Strom, & Myers 1993), but most young clusters are too far away to have their gas structure resolved at the  $0.1 M_{\odot}$  level (Lada et al. 1991; Phelps & Lada 1997). Nevertheless, there is indirect evidence for structure in star-forming cores in the form of extinction fluctuations (Lada et al. 1994; Alves et al. 1998) and a high level of collisional excitation (Falgarone, Phillips, & Walker 1991; Lada, Evans & Falgarone 1997).

The observation of stars in truly structureless cores is not contradictory either. The only thing the model assumes is that the mass which eventually ends up in stars comes originally from the “branches” in a hierarchical tree of gas structure (see Houlahan & Scalo 1992 for a tree-like representation of cloud structure). *When* this selection of pre-stellar masses actually occurs in the life of a cloud does not have to be specified to get the IMF. Indeed, most observations of star-forming cores, particularly those with only one or a few stars, are made at a phase in their evolution that is far removed from the time when they were part of any fractal structure. The cores have already become strongly self-gravitating, rounded, centrally condensed, and dynamically *detached* from the turbulent structure around them (e.g. Myers 1985; Andre,

Ward-Thompson, & Motte 1996), i.e., they may not be fractal anymore. To understand star formation fully, we have to know where these cores came from and what they were like *before* they became strongly self-gravitating. But to understand the IMF in this model, we only have to assume they evolved at constant mass from one of the nodes of a hierarchically structured, younger cloud.

Other theories of the IMF and star formation differ in a significant way from this. Most assume that stars form in uniform clouds, perhaps moving and accreting gas uniformly (e.g., Bonnell et al. 1997), or spontaneously triggered by magnetic or other fluctuations in a uniform or gradually stratified density (Carlberg & Pudritz 1990; Myers 1998). Others assume stars determine their own mass by wind-limited accretion from a uniform medium (Nakano, Hasegawa, & Norman 1995; Adams & Fatuzzo 1996) or by wind-dominated cloud dynamics (Silk 1995). The observation of pervasive clumpy structure with a hierarchical design in pre-stellar clouds (see reviews in Scalo 1985, Falgarone 1989, Elmegreen & Efremov 1998) suggests that these uniform cloud models may have the evolution backwards. Star formation, we assert, is a progression from hierarchical, non-self-gravitating clouds that probably form by turbulent processes at modest pressure in the general interstellar medium, to stellar-mass, centrally-condensed cores that are dominated by gravity. Since the hierarchical structure in pre-stellar clouds goes far below stellar masses (e.g., Heithausen et al. 1998), this evolution necessarily involves *increased smoothing with time* at the stellar mass level. The other models take the opposite approach by trying to generate *increased substructure with time* inside initially smooth clouds.

Our approach, based on increased smoothing in clouds that are already highly structured, may involve several physical processes. One might be the coalescence of non-self-gravitating, sub-stellar clumps into self-gravitating stellar clumps (Whitworth et al. 1998). This preserves hierarchical structure if every clump coalesces with another clump, and it preserves the density dependence for the conversion rate of gas into stars because the collision rate of sub-structures is proportional to the clump crossing rate on all scales (cf. Appendix). Another process might be the progressive loss of magnetic wave coupling to turbulent motions during cloud contraction, as the opacity to ionizing radiation increases and the coupling of charged grains to the magnetic field decreases (Myers & Khersonsky 1995). Perhaps some of the details of the IMF will depend on this evolution, but as long as the probability that a node in the initial hierarchy turns into a star is about the same as that assumed here, namely that it increases slightly with local density, then a Salpeter IMF should result.

## 5. The Model: Variations in the slope of the IMF power law

Scalo (1998) compiled observations of the IMF and plotted the slopes derived by various authors versus the average log mass of the stellar sample. Scalo's diagram is reproduced in Figure 1. The result shows the general change in slope from a value close to 0 in the flat part to a value that hovers around the Salpeter slope of  $-1.35$  (dashed line). These values are for the mass function when it is plotted in equal intervals of the log of the mass; for equal intervals of the mass itself, the slope is about  $-1$  at low mass, and  $-2.35$  at intermediate to high mass. The figure shows the slope of the IMF varies from region to region by about  $\pm 0.5$ . There are typically several hundred stars in each IMF determination (Scalo, private communication).

The average mass range on the abscissa for the samples in figure 1 varies from sample to sample because the total number of stars and the sensitivity of the surveys vary. Generally, the IMF is determined from the most massive stars in a region because these are the only stars that can be seen. If a region has only several hundred stars total, then the most massive star is likely to be small and the average mass

plotted in figure 1 is small. If the region has  $10^4$  stars or more, but is far away and only the brightest stars can be seen, then the average mass plotted in figure 1 is large. The total number of stars in each survey is related to the mass range for the fit. In the power law part of the IMF, with a power  $x = 1.35$  as in the Salpeter IMF, the mass function in equal intervals of mass is  $n(M)dM = n_0 M^{-1-x} dM$ . If the largest star in the region has a mass  $M_L$ , then  $\int_{M_L}^{\infty} n(M)dM = 1$ , giving  $n_0 = xM_L^x$ . Suppose now that the mass range for stars in the fit to the slope is a factor of  $F$ . Then the number of stars used for the fit is  $\int_{M_L/F}^{M_L} n(M)dM = F^x - 1$ . For  $F = 50$  and  $x = 1.35$ , there are  $50^{1.35} - 1 \sim 200$  stars in the sample. Many observational surveys have much smaller  $F$  and number of stars than this.

We fit the IMFs in the models in the same way they were fit in the observations, using only the most massive stars in the sample. The model was run 100 times, with a different number of stars each time, so the most massive star in the sample varies from model to model. We chose a mass range for the slope-fitting region to have its high mass limit less than the mass of the most massive star in the sample by a fixed number of filled histogram bins, equal to 20 bins in the cases shown here, which corresponds to a factor of  $\sim 3$  in mass (the bin spacing is logarithmic in mass). This avoidance of the most massive stars in the ensemble puts us in the power law range, away from obvious statistical fluctuations with a small number of most massive stars. It is what an observer would do with an IMF that has a few “odd” massive stars at the tail end of a smooth power law distribution. Then we systematically decrease the lower mass limit for the fitted region until a fixed total number of stars is reached, which is chosen to be 200 to place us in the range of typical IMF observations. This number, as well as the bin spacing, will be varied to show how the rms fluctuations in the slope of the IMF depend on the number of stars in the sample.

The top left panel in figure 2 shows IMF slopes for 100 random models, each with a different number of stars. The models all have 8 hierarchical levels and an average of 3 sub-clumps per clump (distributed as a Poisson variable – see Paper I). The slopes were all calculated at the high mass ends of the resulting IMF power laws, including 200 stars when there were that many (the lowest mass points have fewer than 200 stars), and excluding the stars in the 20 largest mass bins for each sample, as discussed above. There is considerable scatter at intermediate to high mass in the slope of the IMF around the average value of  $-1.35$ , which is indicated by the dashed line. The average slope increases to zero at low mass, as in the observations, because this is where the IMF flattens out at the thermal Jeans mass (assumed to equal  $0.3 M_{\odot}$  in the model). The slope even increases to slightly positive values at large mass in the model, because a Gaussian probability for failure ( $P_f$  in the notation of paper I) is used, and this causes the IMF to fall at masses lower than the thermal Jeans mass. This positive excursion of the IMF is not a physical result, but is based entirely on this assumption of a Gaussian. Models with an exponential  $P_f$  had slopes increase only to zero, with no positive values. There are no observations of the IMF slope at such low masses anyway, so we have no particular reason to choose one  $P_f$  over any other.

The other panels in figure 2 show the model IMFs for the three cases indicated by crosses in the top left plot. These are three representative cases illustrating how the IMF varies around the mean slope. A case with the mean slope is in the top right, and cases with shallower and steeper slopes are shown in the lower left and right. The total model IMF is shown for each case, along with the subpart that was used to calculate the slope for the 200 bright stars. These subparts are shifted upwards for clarity, once with the same bin size and again with the bins four times wider. The least square fits used for the plotted slopes are shown.

Observations of IMFs like those in the lower left and right of figure 2 might lead one to conclude that the power law in the IMF varies significantly from region to region. However, these are just random fluctuations in the model, both in the geometrical arrangement of the cloud hierarchy, and in the selection

of pieces to make stars.

Figure 3 (left) shows the rms deviations of the model IMF slopes from the average values in the mass range from 1 to  $10 M_{\odot}$  as functions of the number of stars that were used to determine the slopes from each sample. The total numbers of stars in the model clusters were equal to or larger than 1000 for this mass range, ranging from  $10^3$  to  $1.8 \times 10^4$  as average stellar mass increases from  $1 M_{\odot}$  to  $10 M_{\odot}$ . Three different bin spacings for logarithmic mass intervals are represented by three different line types, corresponding to factors of  $3^{1/2}$ , 3, and  $3^2$  in mass for 10 bins. The figure indicates that the rms fluctuations decrease with increasing number of stars in the measurement, independent of bin size; this is a reasonable result for statistical fluctuations. The mean number of stars per IMF fit that is required by the model to give the observed level of fluctuations in real star clusters, namely,  $\pm 0.5$ , is about 80, provided all the scatter in the observed slopes is from statistical sampling. If some of the observed scatter is from measurement errors, which is likely, then the mean number of stars necessary to reproduce the observed scatter could be larger.

The dot-dashed line on the left in figure 3 represents a completely different set of 100 models. These also produce scatter plots like those in figure 2, with the same average IMF slope, but there is an additional statistical variation for this dashed line. This is an addition step in the model that allows the fraction of the clump mass (from the hierarchical tree) that actually goes into a star to vary in a random way. We use a randomly generated mass fraction per clump,  $f$ , that is given by

$$f = \frac{e^{\xi}}{1 + e^{\xi}} \quad (1)$$

where  $\xi$  is a random variable distributed as a Gaussian centered on  $\xi = 0$  with a dispersion of unity. This fraction  $f$  therefore varies between 0 and 1 with a most likely value of 0.5, where  $\xi = 0$ , and  $f$  has a variation around this most likely value ranging from an average of  $e^{-1}/(1 + e^{-1}) = 0.27$  to  $e/(1 + e) = 0.73$ , representing a factor of 2.7 in the local efficiency of star formation. Such an additional random variation seems reasonable for real star formation, but it does not increase the rms variation in the IMF slope in any noticeable way, according to figure 3.

The three lines on the right in figure 3 were generated for the same three bin sizes by randomly sampling points directly from a power law with a slope  $-(1 + x) = -2.35$ . There is no hierarchical cloud structure or selection of cloud pieces as in the IMF model discussed elsewhere in this paper. The point of this diagram is to show the level of statistical fluctuations that are expected from any model of the IMF that produces an average power law with the same slope as in the hierarchical model. As in the other cases, we first generate the stars, and then we select the power law region of the sampled IMF starting a factor of 3 below the largest stellar mass. Obviously, random samples from any model of the IMF will produce fluctuations in the slope when the number of stars is small. It is interesting that these fluctuations are slightly larger for the initial power law than for the IMF that was generated by randomly sampling a hierarchical cloud.

Figure 4 shows 20 model IMFs in the range from 1 to  $10 M_{\odot}$ , selected out of a new sample of 100 random IMFs constructed from hierarchical trees in the usual way. These 100 models were all chosen to have a total number of stars ( $\sim 2400$ ) such that  $\sim 200$  were in the  $1-10 M_{\odot}$  mass range. To make the figure, the power law slopes for the resultant IMFs were evaluated in this mass range, and placed in ascending order. Then every fifth IMF was chosen to get the 20 plotted IMFs. This gives an unbiased choice for presentation that spans the full range of IMFs from these 100 runs. The values of the slopes are shown in each panel. There are 5 bins between 1 and  $10 M_{\odot}$ , to be consistent with the small number usually used by observers; this choice of bins should not affect the slopes (cf. Fig. 3). A histogram of all 100 slopes for

this sample, again evaluated in the  $1-10 M_{\odot}$  mass range, is in figure 5. The dispersion in this histogram is consistent with the value obtained from figure 3 for the cases with 200 stars in the  $1-10 M_{\odot}$  mass interval.

The IMF fluctuations shown in this section represent what should be expected from random variations around a universal IMF. There is no a priori reason to think that the real IMF is universal, but if it is, then slope variations of several tenths, depending on the sample size, are to be expected. If the real IMF is not universal, but has variations in power law slopes that are greater than statistical fluctuations, then additional physics has to be added to the model, or the model is wrong. For example, Scalo (1998) gives examples of well-studied clusters with smooth power law IMFs that vary in slope from  $x = 1.1$  to  $2.3$  (NGC 663 from Phelps & Janes 1993; Pleiades from Meusinger et al. 1996). If these observations reflect the real initial mass functions for the entire clusters, including the outlying stars, and not just the effects of mass segregation, sampling errors, improper evolution corrections, and other problems, then the theoretical model needs revision.

## 6. The Model: Mass-dependent Birth positions

The IMF model in Paper I operates by first generating a random hierarchical tree including a wide range of masses at the various branches, ranging from masses much less than a stellar mass to masses generally larger than the largest star. It then selects branches from this tree randomly and assigns the residual mass on that branch to a new stellar mass that becomes part of the final IMF. This selection of masses is repeated for each star until the original tree has no mass left (or has some fraction of its initial mass left, in an alternative model – see Paper I), and then a new tree is generated and new star selections begin.

The generation of the hierarchical tree was described in detail in Paper I. Now we add positions to this tree, so that each node has a three-dimensional coordinate that is consistent with the fractal dimension of the overall structure. This dimension is assumed to be 2.3, because this is the value we found from a survey of molecular cloud size distributions (Elmegreen & Falgarone 1996), but other values close to this give about the same IMF. The relative positions of the “inner” subclumps inside each “outer” clump are determined by the addition of random offsets to each outer clump position in three dimensions. This offset depends on the level  $h = 0$  to 8 in the hierarchy, scaling as  $L^{-h}$  for scale reduction factor  $L = 1.6123$ , which gives a fractal dimension  $D = \log 3 / \log L = 2.3$ ; here, the 3 in the numerator is the average number of subclumps per clump in the model (other values were also used for models in Paper I, with no significant differences in the resulting IMF).

The spatial distribution of mass for the stars that form in the model is determined entirely from this hierarchical tree structure. As for a real tree, the trunk and massive branches are closer to the center of the distribution of all branches than are the low mass branches. Thus the high mass stars tend to form near the center of the cluster in this model. This is also the sense of the birthplace distribution from observations (Hillenbrand & Hartmann 1998).

Figure 6 shows the number fraction (bottom) and the mass fraction (top) of stars having radii less than the value on the abscissa, for a single IMF model with  $10^5$  stars. This is the type of plot used by Hillenbrand & Hartmann to demonstrate a mass-dependent birth position in Orion. In the left-hand panels, the increase in the number fraction or mass fraction with radius traces out the density structure in the model cloud. The four lines in each plot represent different mass intervals for the stars, as indicated by the figure legend. The lines for the most massive stars rise faster at small radii, indicating that these massive

stars are more centrally condensed than the low mass stars. The effect is very weak, however.

The panels on the right in figure 6 show the same data as the panels on the left, but they are plotted with a distorted coordinate system in which the radius  $R'$  equals the 2.3 power of the undistorted radius  $R$ . This is the type of transformation that would be made by a hierarchical cloud as it becomes centrally condensed by self-gravity to the commonly observed  $R^{-2}$  density distribution of an isothermal sphere. During such a transformation, which presumably occurs before star formation begins, the gas mass is conserved so that

$$\int_0^{R'} n'(r) 4\pi r^2 dr = \int_0^R n(r) 4\pi r^2 dr \quad (2)$$

gives  $R'(R)$ . Before the transformation,  $n(r) \propto r^{D-3}$  around the trunk of the fractal tree (because mass scales with  $R^D$ ). If we set  $n' \propto r^{-2}$ , then  $R' \propto R^D$ .

The model we have in mind here is one in which an interstellar cloud begins its life in a non-self-gravitating state, dominated by turbulence and other processes that give it an internal hierarchical structure down to very small scales. Over time, this cloud contracts in the center as a result of self-gravity and the smallest (sub-stellar) clumps begin to merge to form a few star-forming cores. These cores are assumed to preserve the mass distribution they had from the original hierarchical structure, because they are still part of that structure going to larger scales and because the cloud may continuously regenerate new hierarchical structures and new cores as a result of continued turbulence and other processes, including self-gravity. We get the same IMF as in the original model because the overall cloud topology has not changed, but we get stellar birth locations that are more condensed, reflecting the final state of the gas at the time of star formation. This model is purely phenomenological, but it seems reasonable given the similarities and differences in the structures of diffuse and self-gravitating clouds.

The panels on the right of figure 6 show the distribution of birth positions in the condensed cloud. All the stars are more centrally concentrated than they were in the uncondensed cloud, and the concentration of the most massive stars is more pronounced. How well this agrees with the observations is not clear because Orion is the only case where this effect has been measured, independent of evolutionary effects, and Orion has only a few massive stars. Nevertheless, there is some tendency in hierarchical clouds to have the massive stars born closer to the center than the low mass stars. A study of birth positions similar to that for Orion but for 30 Dor would be more revealing because 30 Dor has more stars.

It may be that real star-forming clouds have a much stronger central concentration of massive stars than than the centrally-condensed cloud model predicts. Then additional physical processes must be involved. This seems likely because the center of a cloud differs from the edge with respect to the density, gravitational potential, and degree of shielding from outside radiation. For example, the protostars near the center could accrete gas at a higher rate and become more massive (Larson 1978, 1982; Zinnecker 1982; Bonnell et al. 1997); they could coalesce more (Larson 1990; Zinnecker et al. 1993; Stahler, Palla, & Ho 1998; Bonnell, Bate, & Zinnecker 1998), or the most massive stars and clumps formed anywhere in the cloud could fall to the center faster because of gas drag (Larson 1990, 1991; Gorti & Bhatt 1995, 1996).

## 7. The Model: Mass-dependent birth order

The birth time of the *first* star that forms in a region with a mass in a logarithmic interval centered around  $M$  should increase as  $M^{1.35}$  if the star formation rate is constant and the IMF is randomly sampled. This is true for any model of the IMF that is based on a random appearance of stars of various masses.

The *average* birth times for stars should be independent of mass in these models, however. The mass dependence for the time of *first* birth arises because the number of stars in a logarithmic interval around  $M$  is proportional to  $M^{-1.35}$  in our model and for a Salpeter IMF. Thus the mean time between birth events for stars of this mass equals the total elapsed time of star formation divided by the number of such stars, and this gives a mean time interval between births  $\propto M^{1.35}$ . The mean delay time before the first birth of a star of mass  $M$  equals the mean time interval between all births of such stars, for a uniform star formation rate. Thus the mean delay time before the first birth of a star in a logarithmic interval around  $M$  increases with  $M^{1.35}$ . As a result, an observer of a real star cluster will notice that the low mass stars generally form before the first intermediate mass stars appear, and these intermediate mass stars appear before the first high mass stars. Yet, for a large enough sample of clusters, the *average* time of appearance of each star is always about half the current age of the region (for a constant and continuing star formation rate).

This statistical effect is strong and should be obvious in an active region. It is analogous to the well-known effect in which larger regions tend to produce larger, most-massive stars (see section I). The timing result follows from our model as well. We computed the IMFs for many clusters and kept track of the time of formation of each star. Unlike the previous models, we did not repopulate the cloud after it exhausted its gas, but just quit when it did, with whatever stars formed. Typically between 200 and 500 stars formed in each cluster with 8 levels in the model hierarchy and 3 subclumps per clump. This is a reasonable size for comparisons with observations.

Figure 7 (left) shows the time of first appearance of a star of a certain mass as a function of that mass, in logarithmic intervals, for all of the stars that formed in 11 computed clusters. Figure 7 (right) shows the same result for 6 clusters. In both cases, the distribution of points is the inverse of the IMF, showing a minimum first time of appearance at the same mass where the IMF peaks, and an increase in the time of appearance on both sides of this minimum where the IMF decreases. Recall that these models use a Gaussian probability of failing to form a star,  $P_f$ , and this is entirely by assumption, so the decrease in the IMF and the increase in the first time of formation at masses less than the peak in the IMF has no observational basis and may not apply to real clouds. We could just as easily have assumed an exponential  $P_f$ , as in some cases of Paper I, and then the first time of formation would level off to a small value at all low masses. The increase in the first time of formation for masses higher than  $0.3 M_\odot$  is a prediction of the model, reflecting entirely the stochastic nature of the distribution of star birth in time. The precise form of this birth order distribution is not known from observations, but we predict it to be proportional to  $M^{1.35}$ .

## 8. The Model: Other IMF cases

In Paper I and for all of the models discussed here so far, we have assumed that the probability of selection of a clump in a hierarchical cloud is proportional to the square root of the local clump density, which is larger at smaller mass because of the nature of this type of structure. As a result, low mass clumps are selected more often than the proportion of their number, and the stellar mass spectrum is slightly steeper than the clump mass spectrum. This is a sensible application of various star formation theories, which suggest that gravitational processes, magnetic diffusion, turbulent decay, and coalescence all contribute in some fashion to the local rate of conversion of gas into stars. Considering the molecular cloud scaling laws, all of these processes operate on a timescale that scales approximately with the inverse square root of the local density (see Appendix).

Other models are possible. For example, the conversion rate from non-self-gravitating clumps to

self-gravitating clumps that eventually make stars might be independent of density. We showed in Paper I that this gives an IMF with too shallow a slope,  $-(1+x) \sim -2$  instead of  $-2.35$ , but we can tune the model by selecting only a fraction of the chosen clump mass to go into the star. This is done by letting the star mass,  $M_s$ , equal the chosen gas clump mass,  $M_c$ , raised to some power,  $1-\alpha$ , so the *local* efficiency of star formation, calculated on a star-by-star basis, is

$$\frac{M_s}{M_c} \propto \left( \frac{M_c}{M_J} \right)^{-\alpha} \quad (3)$$

for characteristic thermal Jeans mass,  $M_J$ , which is the mass at the peak of the IMF.

Figure 8 shows the IMFs from three models with  $\alpha = 0.2, 0.4$ , and  $0.6$ ; larger values have steeper slopes. The actual slopes can be calculated by converting the protostellar cloud distribution  $n(M_c)d\log M_c \propto M_c^{-x}d\log M$  into a star distribution  $n(M_s)d\log M_s$  as follows:

$$n(M_s) = n(M_c) \frac{d\log M_c}{d\log M_s} \propto M_c^{-x} = M_s^{\frac{-x}{1-\alpha}}. \quad (4)$$

For  $\alpha = 0.2, 0.4$  and  $0.6$ , with  $x = 1$  in this case, the slope of the IMF becomes  $-1.25, -1.67$ , and  $-2.5$ , in agreement with the results in the figure. Thus the Salpeter IMF can be recovered even in the case where there is a uniform selection probability per level, by choosing  $\alpha = 0.3$ . Similarly, the steep IMF seen by Massey et al. (1995), which has  $x \sim 4$ , can come from our usual Salpeter model ( $x = 1.3$ ) if  $\alpha = 2.7$ .

These solutions are not particularly enlightening because the introduction of an additional parameter has no firm observational basis. Theoretical work on a variable local efficiency has been considered elsewhere (e.g., Zinnecker 1989; Nakano, Hasegawa & Norman 1995; Adams & Fatuzzo 1996). We show the application of this concept here only to emphasize that in our model, the underlying gas mass spectrum that has to be modified by a variable local efficiency has  $x \sim 1.3$ , which is much steeper than the usual clump mass spectrum measured in molecular cloud surveys, which have  $x \sim 0.5 - 0.7$  for logarithmic intervals of  $M$ . Thus any “corrections” that might be introduced to convert the gas mass spectrum to a star mass spectrum are much smaller in our model than in standard models.

If the density dependence of the selection rate differs from both powers  $0$  and  $0.5$ , then the IMF can still be estimated from the basic assumptions of the model. Suppose the selection rate scales with density as  $\omega \propto \rho^\alpha$ . The density scales with mass as  $M^{1-3/D}$ , so the mass dependence of the selection rate scales as  $M^{\alpha(1-3/D)}$ . This mass function directly multiplies the IMF. For  $\alpha = 0.5$  and  $D = 2.3$ , as in the standard case considered for this model, the selection rate  $\propto M^{-0.15}$ , so the IMF is  $M^{-2.15}$  without competition for mass, and it steepens to  $M^{-2.3}$  with competition for mass. Evidently, larger  $\alpha$  makes the IMF steeper.

## 9. Conclusions

A model for the initial stellar mass function based on random selection of gas pieces in a hierarchical cloud, with a selection probability proportional to the square root of density and a lower mass cutoff from the lack of self-gravity, has been shown here and in Paper I to reproduce six features of the observed IMF: (1) the power law slope and its remarkable constancy from place to place over the history of the Universe, (2) the low mass flattening at about the thermal Jeans mass, (3) the constancy of this thermal Jeans mass from place to place and over time in normal star-formation environments, and its increase in starburst regions, (4) the seemingly random fluctuations in the power-law slope from region to region, (5) the tendency for higher mass clusters and clouds to form higher mass stars, and (6) the tendency for high

mass stars to form more centrally condensed in clusters and at later times than low mass stars. The only physical scale involved in any of these processes is the thermal Jean mass, which is about  $0.3 M_{\odot}$  in the solar neighborhood for typical temperatures and pressures in star-forming clouds (Paper I).

Reasonable modifications to this theory make it more realistic in terms of star formation processes, but should not affect the resulting IMF. For example, star-forming clouds may evolve from a previous diffuse state by simple contraction, or perhaps by high-pressure, forced rearrangement (e.g., triggering), to form centralized concentrations that have essentially the same hierarchical structure as the original cloud, although the condensed version is not self-similar anymore and the individual clumps may have redistributed their gas. Nevertheless, as long as the stars form in clumps that come from many different levels in the hierarchy, the Salpeter IMF will result.

Another implication of the model is that the individual cores in which single or binary stars form must have grown from lower mass clumps as a result of various smoothing processes that counteract the tendency for turbulence to subdivide. In this sense, our model differs significantly from most other IMF models, which attempt to partition initially uniform gas into stellar-mass pieces. Our starting point is the observation by several groups that hierarchical structure and power-law mass distributions continue down to sub-stellar scales in pre-star-formation clouds.

Additional observations and experimental tests of the model were proposed. Any direct observation of cluster-to-cluster variations in the mass at which the IMF changes from the power law part to the flat (or even turnover) part would give us a better idea of whether or not this characteristic mass is the thermal Jeans mass, depending exclusively on the square of the gas temperature and the inverse square root of the cloud-core pressure. More observations of the radial distributions of various stellar masses in clusters are also necessary to determine whether the physical processes of star formation change significantly in the cloud core. We would also like to know whether deviations from a Salpeter IMF in clusters ever exceed the statistical expectations from the theory, given the number of stars observed.

These and other tests are useful because they are based on observations of stars rather than gas, so they represent a known state in the evolution of the star-forming region. Observations of the gas have a problem in not knowing this evolutionary state, e.g., whether a relatively smooth, centrally condensed clump in which a star is currently forming came from the fragmentation of an even larger, but smooth, gas distribution, or the blending together of much smaller structure that was made by turbulence. Observations of the gas also suffer from resolution limitations and chemical selection effects. There is also a tendency, when observing the gas, to overlook the wide variety of processes that are likely to contribute to star formation, concentrating instead on the boundary and other conditions of the particular cloud under investigation. Such conditions are essential for understanding the star formation process itself, but they may not be necessary for understanding the IMF, which is a highly reduced average of all possible outcomes.

## 10. Appendix

The time scales for many processes connected with star formation are roughly proportional to the inverse square root of the local density. This is obviously true for self-gravitational processes, which operate on the time scale  $(G\rho)^{-1/2}$  for local density  $\rho$ . It is also true for magnetic diffusion when the gas is in equipartition between magnetic and self-gravitational forces, or between magnetic, turbulent and self-gravitational forces, because then the diffusion time is a constant of order 10 times the gravity time (for detailed models of this, see Elmegreen 1979 or Nakano 1998, and references therein; for a general review,

see Shu, Adams & Lizano 1987).

Turbulent processes work on the same time scale. The turbulent crossing time is  $L/v$  for length scale  $L$  and turbulent speed  $v$ , but the scaling relationships for molecular clouds (Larson 1981; Solomon et al. 1987) give  $v \sim L^{1/2}$  and  $\rho \propto L^{-1}$ , so  $L/v \propto \rho^{-1/2}$ . For clouds in equipartition between magnetic, turbulent and self-gravitational forces, the constant of proportionality here is about the same as that for gravitational processes.

Collisions between subclumps at each level also have a time scale of about one crossing time on the scale of the larger clump in which they are clustered. If the “internal” subclump sizes are  $L_i$ , the size of the “external” clump that contains them is  $L_e$ , and the turbulent speed on the external scale is  $v_e$ , then the collision time of the subclumps inside each clump is  $t_{col} \sim (n_i \pi L_i^2 v_e)^{-1}$  for subclump density  $n_i = N_i / L_e^3$  and subclump number  $N_i$ . Substituting this expression for  $n_i$ , we get  $t_{col} \sim (N_i \pi L_i^2 / L_e^2)^{-1} L_e / v_e$ . For a fractal cloud,  $N_i = (L_e / L_i)^D$  with fractal dimension  $D$ , thus  $t_{col}$  equals  $(L_i / L_e)^{D-2} / \pi$  times the crossing time,  $L_e / v_e$ . If the hierarchical structure is geometrically self-similar, then  $(L_i / L_e)^{D-2}$  is constant for each clump and equal to  $N_i^{-(D-2)/D} \sim N_i^{-0.13}$  for  $D = 2.3$ . Considering  $N_i \sim 3$  in our IMF models, this is 0.87. Thus the collision time of internal clumps is about equal to the crossing time of the external clump that contains them, and this is true for all scales. This time is also approximately  $(G\rho)^{-1/2}$  when the clumps are virialized.

Helpful comments from John Scalo are greatly appreciated.

## REFERENCES

Adams, F.C., & Fatuzzo, M. 1996, ApJ, 464, 256  
 Ali, B., & DePoy, D.L. 1995, AJ, 109, 709  
 Alves, J., Lada, C.J., Lada, E.A., Kenyon, S.J., & Phelps, R. 1998, ApJ, in press  
 Andre, P., Ward-Thompson, D., & Motte, F. 1996, A&A, 314, 325  
 Bazell, D., & Désert, F.X. 1988, ApJ, 333, 353  
 Beech, M. 1987, Ap&SS, 133, 193  
 Bonnell, I.A., Bate, M.R., Clarke, C.J., & Pringle, J.E. 1997, MNRAS, 285, 201  
 Bonnell, I.A., & Davies, M.B. 1998, MNRAS, 295, 691  
 Bonnell, I.A., Bate, M.R., & Zinnecker, H. 1998, MNRAS, 298, 93  
 Brown, A. G. A. 1998, in The Stellar Initial Mass Function, ed. G. Gilmore, I. Parry, & S. Ryan, Cambridge: Cambridge University Press, p. 45  
 Cayrel, R. 1990 in Physical Processes in Fragmentation and Star Formation, eds. R. Capuzzo-Dolcetta, C. Chiosi & A. Di Fazio, Dordrecht:Kluwer, p. 343.  
 Calzetti, D. 1997, AJ, 113, 162  
 Carlberg, R.G., & Pudritz, R.E. 1990, MNRAS, 247, 253  
 Clarke, C. 1998, in The Stellar Initial Mass Function, eds. G. Gilmore, I. Parry, & S. Ryan, p. 189.  
 Cool, A.M. 1998, in The Stellar Initial Mass Function, ed. G. Gilmore, I. Parry, & S. Ryan, Cambridge: Cambridge University Press, p. 139

Devereux, N. A., 1989, *ApJ*, 346, 126

Dickman, R.L., Horvath, M.A., & Margulis, M. 1990, *ApJ*, 365, 586

Doane, J.S., & Matthews, W.G. 1993, *ApJ*, 419, 573

Doyon, R., Joseph, R.D., & Wright, G.S. 1994, *ApJ*, 421, 101

Eggen, O.J. 1976, *Quart. J. roy. Astron.Soc.*, Vol 17

Eggen, O.J. 1978, *PASP*, 89, 187

Elmegreen, B.G. 1978, *The Moon and the Planets*, 19, 159

Elmegreen, B.G. 1979, *ApJ*, 232, 729

Elmegreen, B.G. 1983, *MNRAS*, 203, 1011

Elmegreen, B.G. 1997, *ApJ*, 486, 944 (Paper I)

Elmegreen, B.G. 1998, in *Origins of Galaxies, Stars, Planets and Life*, ed. C.E. Woodward, H.A. Thronson, & M. Shull, San Francisco, ASP conference series, Vol 148, p. 150

Elmegreen, B.G., & Falgarone, E. 1996, *ApJ*, 471, 816

Elmegreen, B.G., & Efremov, Y.N. 1998, in *The Orion Complex Revisited*, ed. M. J. McCaughrean & A. Burkert, ASP Conference Series, 1998, in press

Falgarone, E. 1989, in *Structure and Dynamics of the Interstellar Medium*, ed. Tenorio-Tagle, G., Moles, M., & Melnick, J. (Berlin: Springer), p. 68

Falgarone, E., Phillips, T.G., & Walker, C.K. 1991, *ApJ*, 378, 186

Falgarone, E., Puget, J.L., & Perault, M. 1992, *A&A*, 257, 715

Falgarone, E., & Phillips, T.G. 1996, *ApJ*, 472, 191

Fischer, P., Pryor, C., Murray, S., Mateo, M., & Richtler, T. 1998, *AJ*, 115, 592

Fleck, R.C., Jr. 1996, *ApJ*, 458, 739

Gorti, U., & Bhatt, H. C. 1995, *MNRAS*, 272, 61

Gorti, U., & Bhatt, H. C. 1996, *MNRAS*, 278, 611

Güsten, R., & Mezger, P.G. 1983, in *Vistas Astr.* 26, 159

Heithausen, A., Bensch, F., Stutzki, J., Falgarone, E. & Panis, J. F. 1998, *A&A*, 331, 65

Henriksen, R.N. 1986, *ApJ*, 310, 189

— 1991, *ApJ*, 377, 500

Herbig, G.H. 1962, *ApJ*, 135, 736

Hetem, A., Jr., & Lepine, J.R.D. 1993, *A&A*, 270, 451

Hillenbrand, L.A. 1997, 113, 1733

Hillenbrand, L.A., & Hartmann, L. 1998, *ApJ*, 492, 540

Hill, J.K., Isensee, J.E., Cornett, R.H., Bohlin, R.C., O'Connell, R.W., Roberts, M.S., Smith, A.M., & Stecher, T.P. 1994, *ApJ*, 425, 122

Hill, R.S., Cheng, K.-P., Bohlin, R.C., O'Connell, R.W., Roberts, M.S., Smith, A.M., & Stecher, T.P. 1995, *ApJ*, 446, 622

Houlihan, P. & Scalo, J. 1992, *ApJ*, 393, 172

Iben I., Jr. & Talbot, R.J. 1966, *ApJ*, 144, 968

Jones, B. F. & Walker, M. F. 1988, *AJ*, 95, 1755

Kennicutt, R.C. 1998, *ApJ*, 498, 541

Khersonsky, V.K. 1997, *ApJ*, 475, 594

Kontizas, M., Hatzidimitriou, D., Bellas-Velidis, I., Gouliermis, D., Kontizas, E., and Cannon, R. D. 1998, *A&A*, 336, 503

Kroupa, P., Tout, C.A., & Gilmore, G. 1990, *MNRAS*, 244, 76

Kulsrud, R., & Pearce, W.P. 1969, *ApJ*, 156, 445

Lada, C.J., Lada, E.A., Clemens, D.P., & Bally, J. 1994, *ApJ*, 429, 694

Lada, E.A., Strom, K.M., & Myers, P.C. 1993, in *Protostars and Planets III*, ed. E.H. Levy & J.I. Lunine, Tucson: Univ. of Arizona Press, p. 245

Lada, E.A., DePoy, D.L., Evans, N.J., II., & Gatley, I. 1991, *ApJ*, 371, 171

Lada, E.A., Evans, N.J., II., & Falgarone, E. 1997, *ApJ*, 488, 286

Lada, E.A., Lada, C.J., & Muench, A. 1998, in *The Stellar Initial Mass Function*, ed. G. Gilmore, I. Parry, & S. Ryan, Cambridge: Cambridge University Press, p. 107

Larson, R.B. 1977, in *the Evolution of Galaxies and Stellar Populations*, ed. B.M. Tinsley & R.B. Larson, Yale University Observatory, p. 97

Larson, R.B. 1978, *MNRAS*, 184, 69

Larson, R.B. 1981, *MNRAS*, 194, 809

Larson, R.B. 1982, *MNRAS*, 200, 159

Larson, R.B. 1986, *MNRAS*, 218, 409

Larson, R.B. 1990, in *Physical processes in fragmentation and star formation*, eds. R. Capuzzo-Dolcetta, C. Chiosi & A. Di Fazio, Dordrecht: Kluwer, p. 389

Larson, R. B. 1991, in *Fragmentation of Molecular Clouds and Star Formation*, ed. E. Falgarone, F. Boulanger, & G. Duvert, Dordrecht: Kluwer, p. 261

Larson, R.B. 1992, *MNRAS*, 256, 641

Leitherer, C. 1998, in *The Stellar Initial Mass Function*, ed. G. Gilmore, I. Parry, & S. Ryan, Cambridge: Cambridge University Press, p. 61

Maddalena, R.J., & Thaddeus, P. 1985, *ApJ*, 294, 231

Massey, P., Lang, C.C., DeGioia-Eastwood, K., & Garmany, C.D. 1995, *ApJ*, 438, 188

Massey, P. 1998, in *The Stellar Initial Mass Function*, ed. G. Gilmore, I. Parry, & S. Ryan, Cambridge: Cambridge University Press, p. 17

Massey, P., & Hunter, D. 1998, *ApJ*, 493, 180

Mezger, P.G., & Smith, L.F. 1977, in *Star Formation*, ed. T. de Jong & A. Maeder, Dordrecht: Reidel, p. 133

Meusinger, H., Schilbach, E., & Souchay, J. 1996, *A&A*, 312, 833

Miller, G.E., & Scalo, J. 1979, *ApJS*, 41, 513

Myers, P.C. 1985, in *Protostars and Planets II*, ed. D.C. Black and M.S. Matthews, Tucson: Univ. of Arizona Press, p. 81

Myers, P.C. 1998, *ApJ*, 496, L109

Myers, P.C., & Khersonsky, V.K. 1995, *ApJ*, 442, 186

Nakamura, F., Hanawa, T., & Nakano, T. 1995, *ApJ*, 444, 770

Neufeld, D.A., Lepp, S., & Melnick, G.J., 1995, *ApJS*, 100, 132

Nakano, T. 1998, *ApJ*, 494, 587

Nakano, T., Hasegawa, T., & Norman, C. 1995, *ApJ*, 450, 183

Nota, A. 1998, in *Unsolved Problems in Stellar Evolution*, poster paper.

Pandey, A. K., Mahra, H. S., & Sagar, R. 1992, *Astr.Soc.India*, 20, 287

Parker, J. W., Hill, J. K., Cornett, R. H., Hollis, J., Zamkoff, E., Bohlin, R. C., O'Connell, R. W., Neff, S. G., Roberts, M. S., Smith, A. M., & Stecher, T. P. 1998, *AJ*, 116, 180.

Pfenniger, D. & Combes, F. 1994, *A&A*, 285, 94

Phelps, R.L., & Janes, K. A. 1993, *AJ*, 106, 1870

Phelps, R.L., & Lada, E.A. 1997, *ApJ*, 477, 176

Reid, N. 1998, in *The Stellar Initial Mass Function*, ed. G. Gilmore, I. Parry, & S. Ryan, Cambridge: Cambridge University Press, p. 121

Rieke, G.H., Lebofsky, M.J., Thompson, R.I., Low, F.J., & Tokunaga, A.T. 1980, *ApJ*, 238, 24

Rieke, G.H., Loken, K., Rieke, M.J., Tamblyn, P. 1993, *AJ*, 412, 99

Sagar, R., & Bhatt, H. C. 1989, *J.Ap.Astron.*, 10, 173

Salpeter, E.E. 1955, *ApJ*, 121, 161

Satyapal, S., et al. 1995, *ApJ*, 448, 611

Satyapal, S., et al. 1997, *ApJ*, 483, 148

Scalo, J.M. 1985 in *Protostars and Planets II*, ed. D.C. Black & M.S. Mathews (Tucson: Univ. of Arizona Press), 201

Scalo, J.M. 1986, *Fund.Cos.Phys*, 11, 1

Scalo, J.M. 1990a, in *Windows on Galaxies*, ed. A. Renzini, G. Fabbiano, & J.S. Gallagher, Dordrecht: Kluwer, 125

Scalo, J. 1990b in *Physical Processes in Fragmentation and Star Formation*, eds. R. Capuzzo-Dolcetta, C. Chiosi, & A. Di Fazio (Dordrecht: Kluwer), p. 151

Scalo, J.S. 1998, in *The Stellar Initial Mass Function*, ed. G. Gilmore, I. Parry, & S. Ryan, Cambridge: Cambridge University Press, p. 201

Schaerer, D. 1996, *ApJ*, 467, L17

Shu, F.H., Adams, F.C., & Lizano, S. 1987, *ARA&A*, 25, 23

Silk, J. 1995, *ApJ*, 438, L41

Smith, D.A., Herter, T., Haynes, M.P., Beichman, C.A., & Gautier, T.N., III 1995, *ApJ*, 439, 623

Solomon, P.M., Rivolo, A.R., Barrett, J., & Yahil, A. 1987, *ApJ*, 319, 730

Sreenivasan, K.R. 1991, *Ann. Rev. Fluid Mech.*, 1991, 23, 539

Stahler, S. W., Palla, F., & Ho, P. T. P. 1998, in *Protostars and Planets IV*, eds. A. P. Boss & S. S. Russell, Tucson: Univ. Arizona Press, in press.

Stutzki, J., Bensch, F., Heithausen, A., Ossenkopf, V., & Zielinsky, M. 1998, *A&A*, 336, 697

Telesco, C.M. 1988, *ARA&A*, 26, 343

Tomisaka, K. 1996, *PASJ*, 48, 701

Tsujimoto, T., Yoshii, Y., Nomoto, K., Matteucci, F., Thielemann, F.-K., & Hashimoto, M. 1997, *ApJ*, 483, 228

Vazquez, R. A., Baume, G., Feinstein, A., & Prado, P. 1996, *A&A*, 116, 75

Vogelaar, M.G.R., & Wakker, B.P. 1994, *A&A*, 291, 557

Whitworth, A.P., Boffin, H.M.J., & Francis, N. 1998, *MNRAS*, 299, 554

Wright, G.S., Joseph, R.D., Robertson, N.A., James, P.A., and Meikle, W.P.S. 1988, *MNRAS*, 233, 1

Wyse, R.F.G. 1998, in *The Stellar Initial Mass Function*, ed. G. Gilmore, I. Parry, & S. Ryan, Cambridge: Cambridge University Press, p.89

Zimmermann, T. & Stutzki, J. 1992, *Physica A*, 191, 79

Zimmermann, T. & Stutzki, J. 1993, *Fractals*, 1, 930

Zinnecker, H. 1982, in *Symposium on the Orion Nebula to honor Henry Draper*, eds. A. E. Glassgold, P. J. Huggins, & E. L. Schucking, New York: New York Academy of Science, p. 226

Zinnecker, H. 1989, in *Evolutionary Phenomena in galaxies*, eds. J.E. Beckman, & B.E.J. Pagel, Cambridge: Cambridge Univ. Press, p. 113

Zinnecker, H., McCaughrean, M. J., Wilking, B. A. 1993, in *Protostars and Planets III*, eds. E. H. Levy & J. I. Lunine, Tucson: Univ. Arizona, p. 429

Zinnecker, H. 1996, in *The Interplay between Massive Star Formation, the ISM, and Galaxy Evolution*, ed. D. Kunth et al. (Gif-sur-Yvette: Editions Frontieres), p. 151

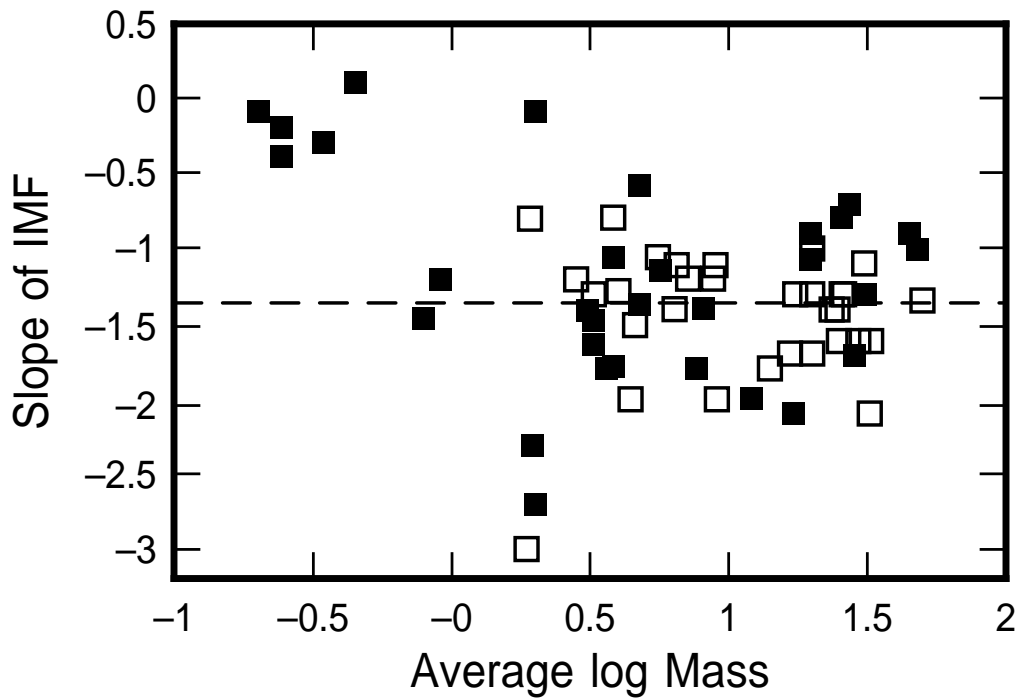


Fig. 1.— IMF slopes in different clusters as a function of the average log mass, in  $M_{\odot}$ , from Scalo (1998). The Salpeter value of  $-1.35$  is shown by a dashed line. Solid squares are for clusters in the Milky Way, and open squares are for the Large Magellanic Cloud.

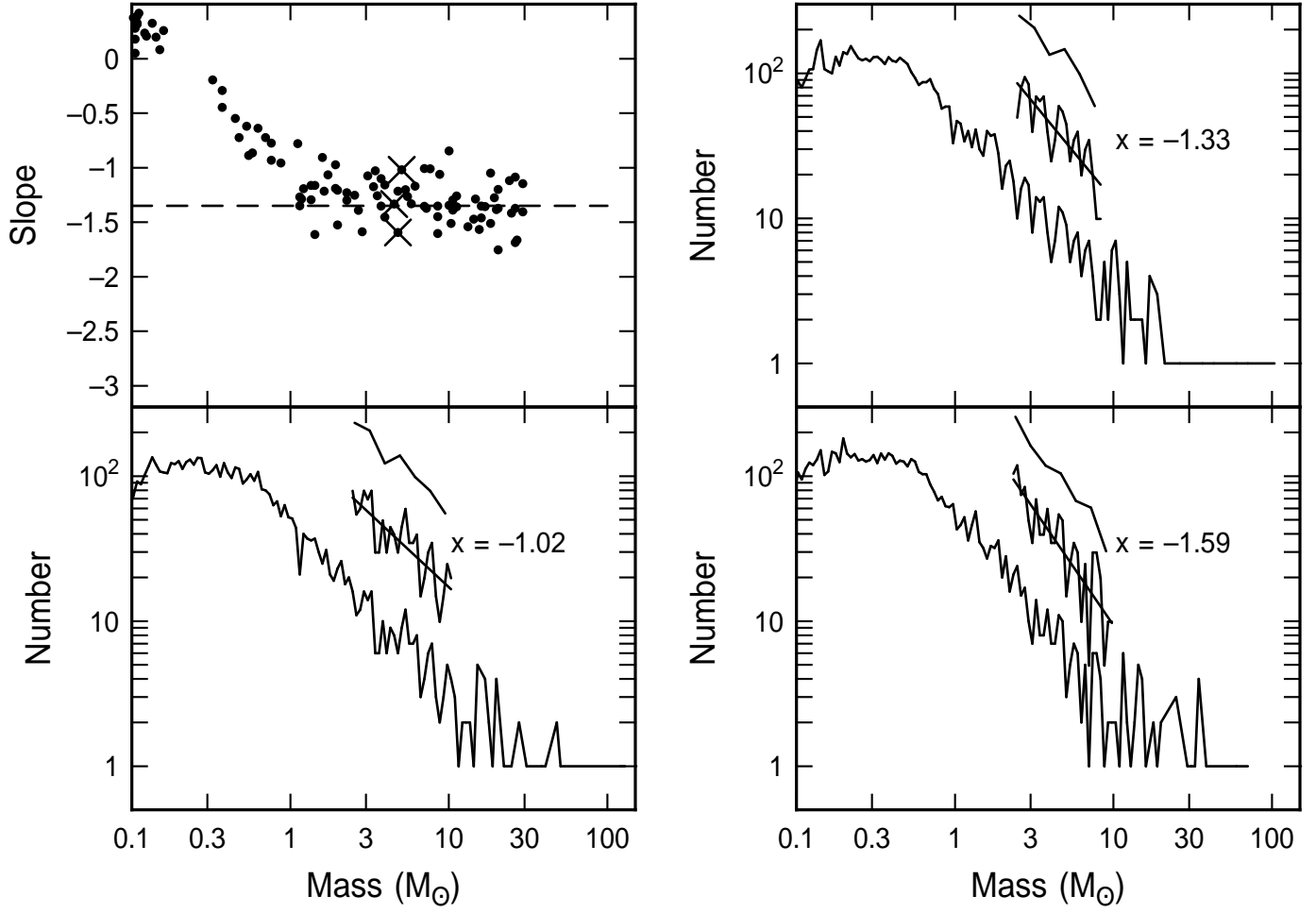


Fig. 2.— (top left) IMF slopes in 100 models that differ in the sequence of random numbers used to generate and sample the fractal cloud tree, plotted as a function of the average logarithm of the mass, as in Fig. 1. Each IMF slope is fit using 200 stars, with the largest star in the fit taken to be smaller by 20 filled mass bins than the largest star produced in the model. The Salpeter value of  $-1.35$  is shown by a dashed line. The three values indicated by crosses have their complete IMFs shown in the other panels. The fitted portions of these IMFs are indicated by the offsets, with two different bin sizes shown.

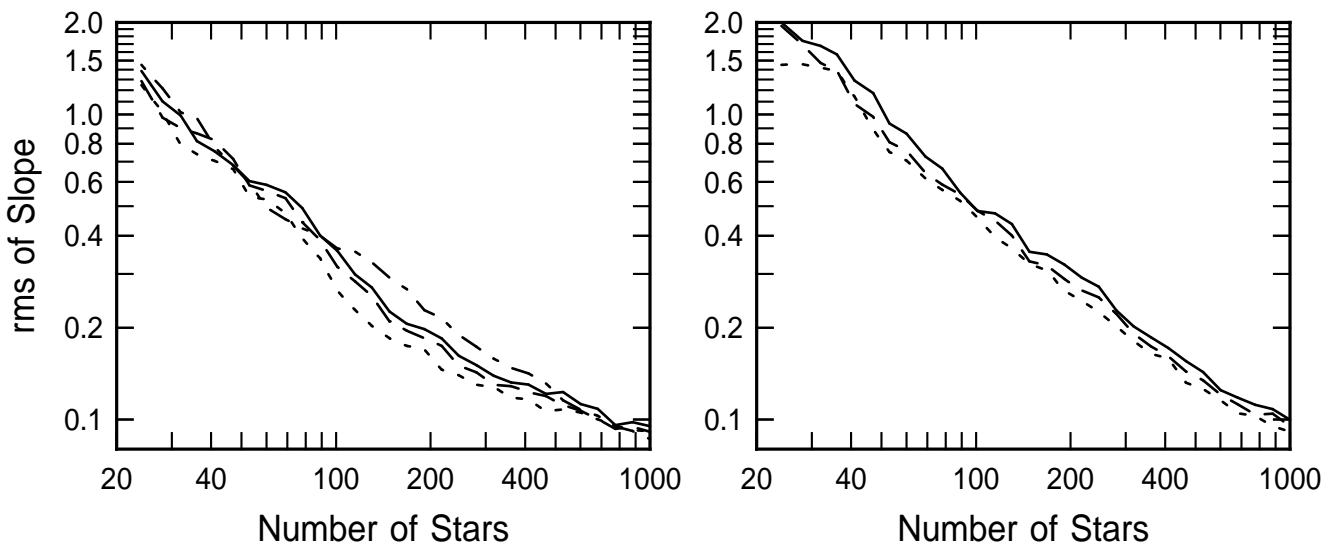


Fig. 3.— (left) The rms deviation in the fitted slopes of the model IMFs for the  $1-10 M_{\odot}$  range, plotted versus the number of stars that are included in the fit. The solid line is for the case shown in Fig. 2, the dashed line has twice the bin size, and the dotted line has four times the bin size. The dot-dashed line is for another 100 independent IMFs that have an additional randomness in the ratio of the star mass to the clump mass. This figure shows that the model IMF converges to a universal power law as the number of stars in the cluster increases. (right) The rms deviations are shown for three bin sizes in a model where a power-law IMF is sampled randomly, without any consideration of how the power law arises.

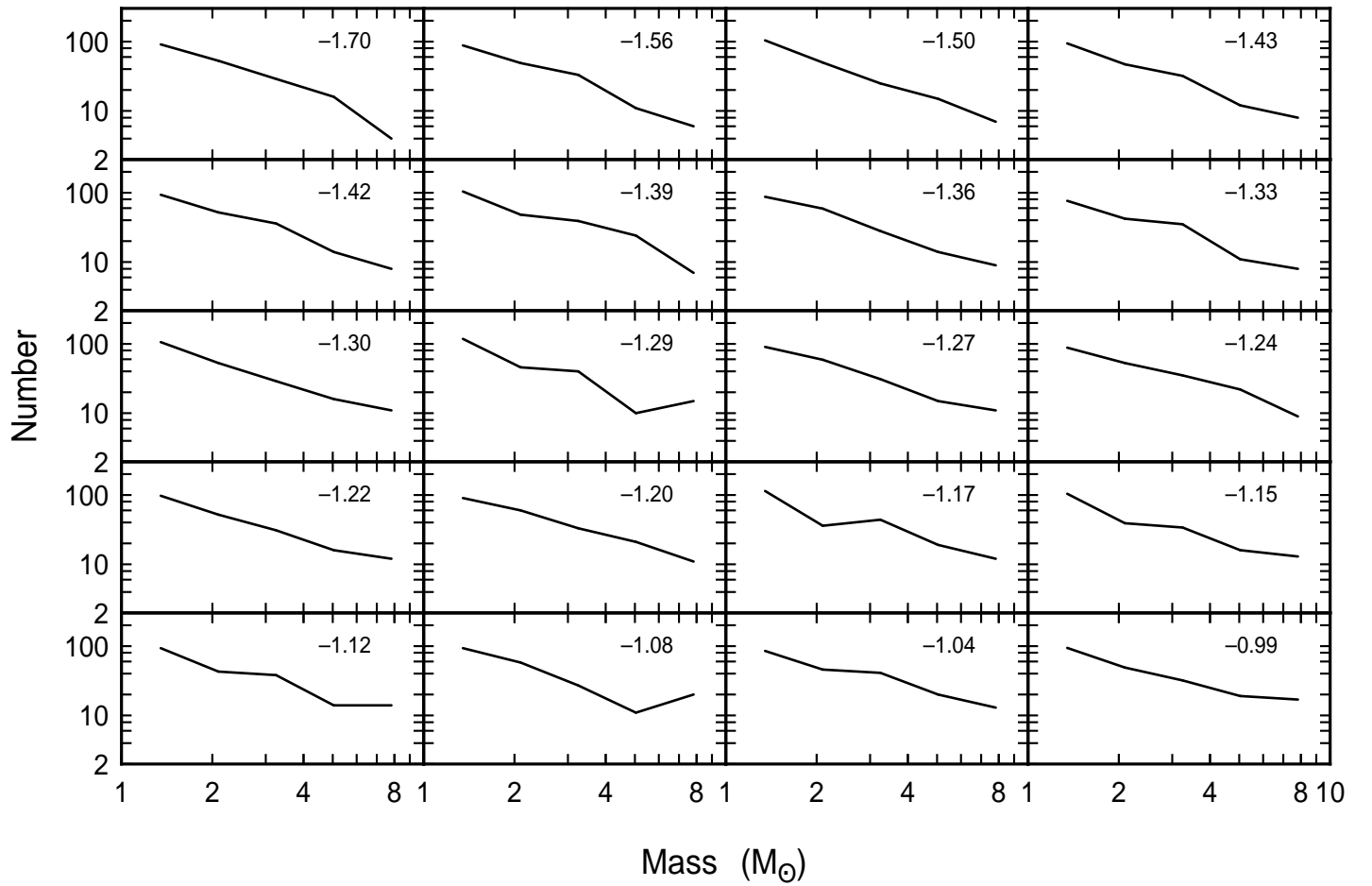


Fig. 4.— (left) The IMFs from 20 out of 100 runs, selected in a regular and unbiased way to represent the full range of slopes, along with values of the slopes in each panel, evaluated in the mass range from 1 to 10  $M_{\odot}$ .

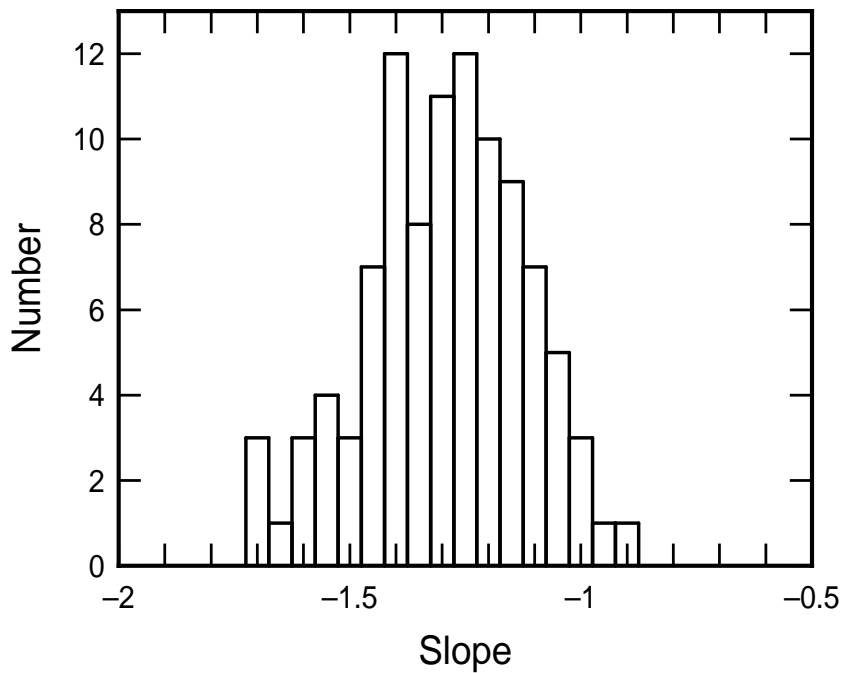


Fig. 5.— (left) Histogram of 100 slopes in the mass range from 1 to  $10 M_{\odot}$  for 100 standard IMF models.

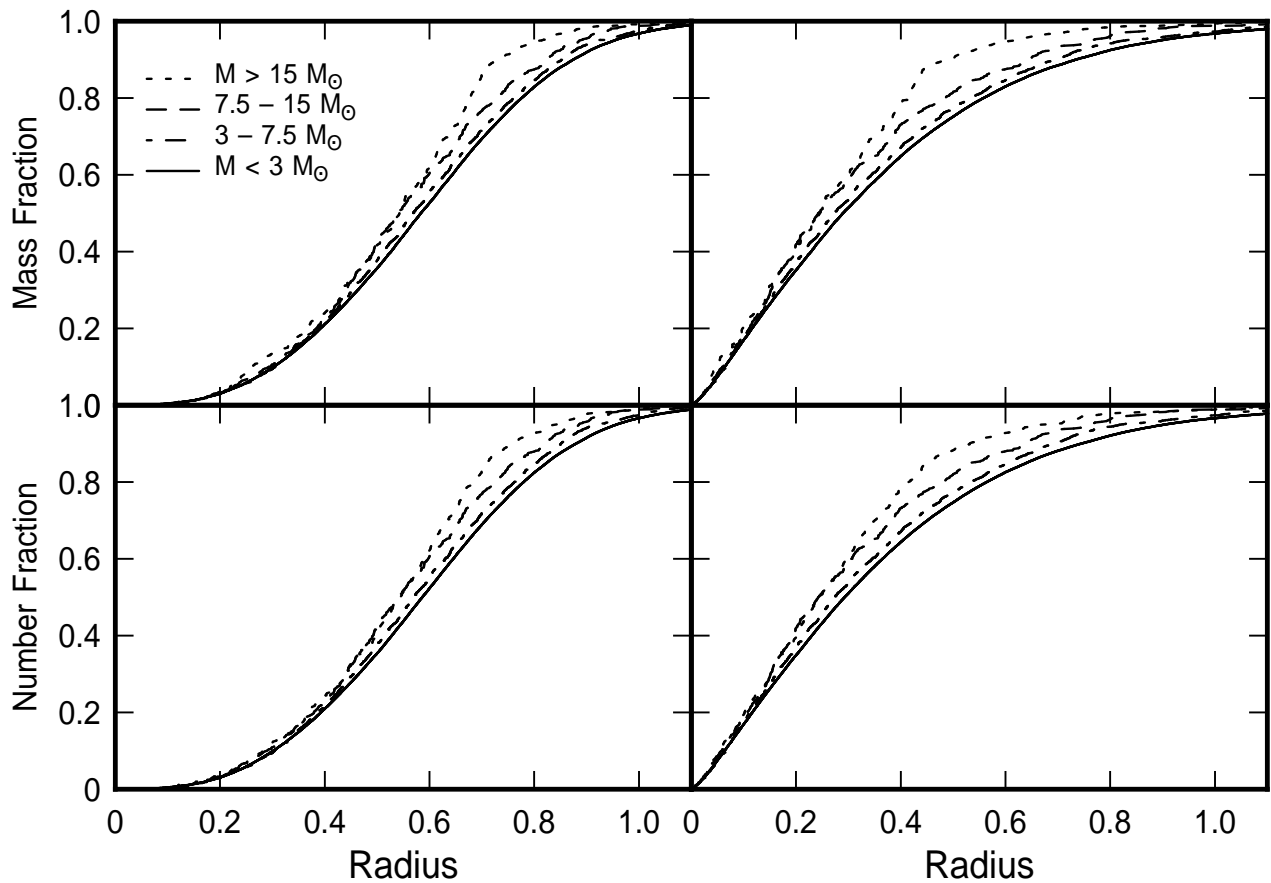


Fig. 6.— The average birthplaces of stars with various masses are shown as cumulative functions of the number fraction and mass fraction within a certain radius. The panels on the left are for the pure fractal model, and the panels on the right are for a distorted fractal with a density profile like that of a molecular core. The massive stars are born slightly closer to the center than the low mass stars.

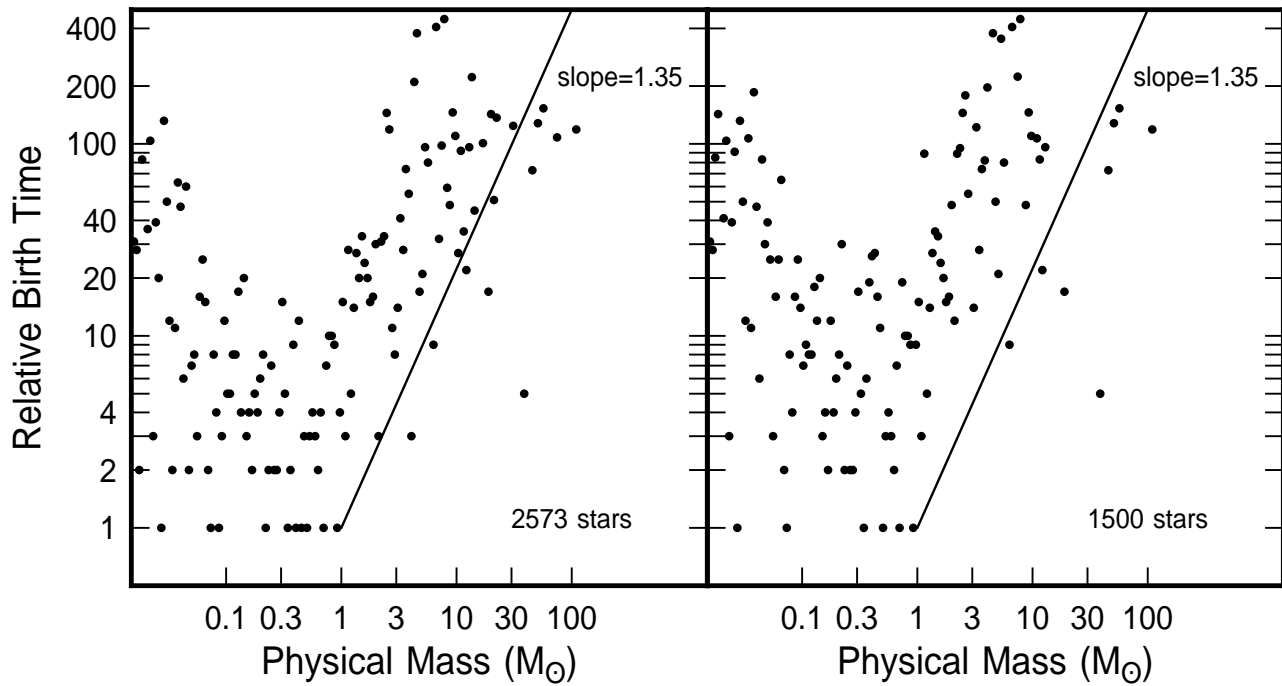


Fig. 7.— The relative birth time for the first appearance of a star with a certain mass is shown as a function of that mass for a composite of 11 clusters on the left, containing 2573 stars total, and 6 clusters on the right, containing 1500 stars. The relative birth time is measured in units of the time of first appearance of any star in the model. The dots with relative birth times of 1 are the first masses that appear in the 11 or 6 clusters. The dots with large relative birth times are for masses whose first appearance was late in every cluster. The solid line has a slope of 1.35, indicating the theoretical prediction. Massive stars tend to form late in a cluster because they are rare. Thus the relative birth time has a distribution with mass that is the inverse of the IMF.

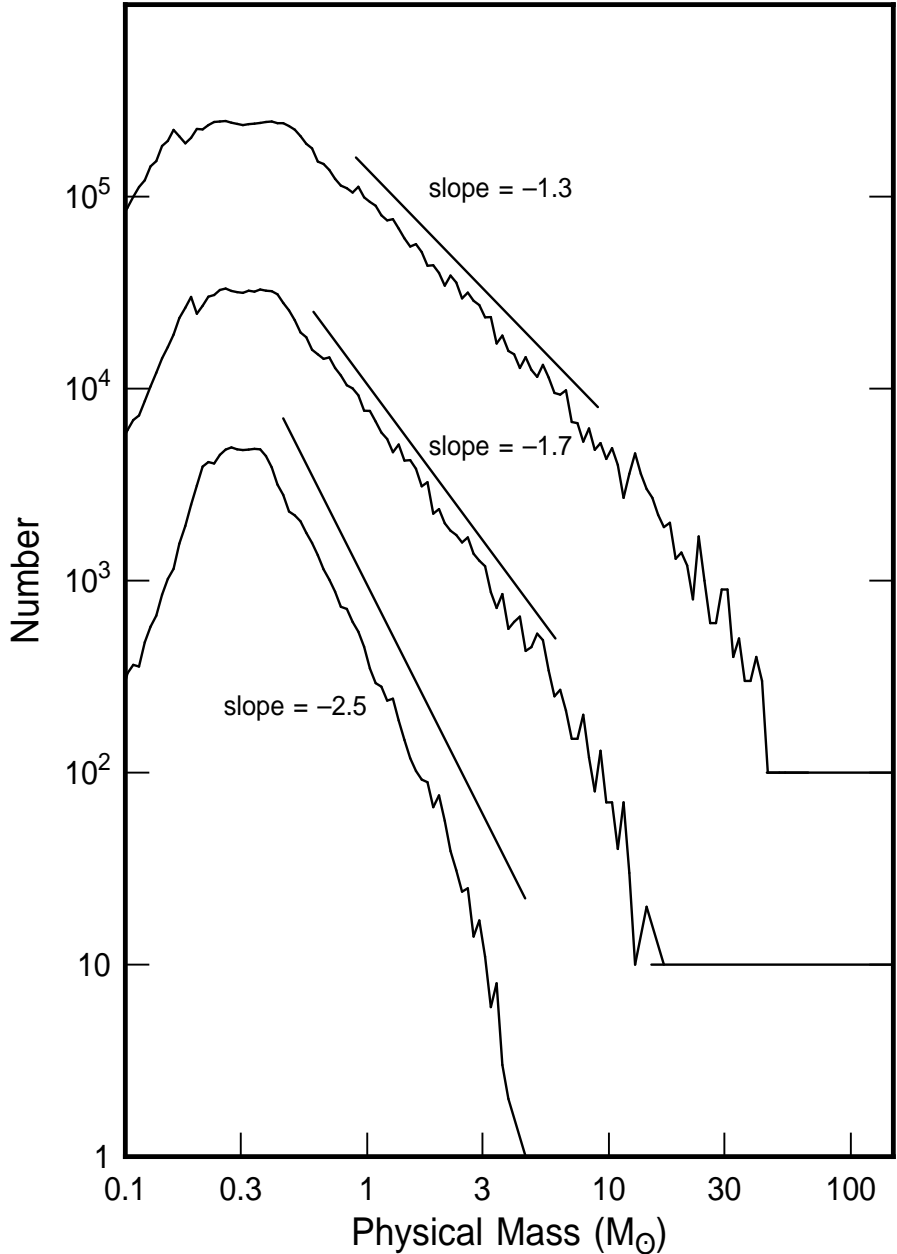


Fig. 8.— Three model IMFs using  $10^5$  stars are shown with different power law distributions of the local efficiency,  $M_s/M_c \propto M_c^{-\alpha}$ , for  $\alpha = 0.2$  on the top, 0.4 in the middle, and 0.6 at the bottom. The solid lines show the predicted slopes. The bottom IMF has the proper number given on the ordinate, while the top two IMFs are shifted upwards for clarity.